

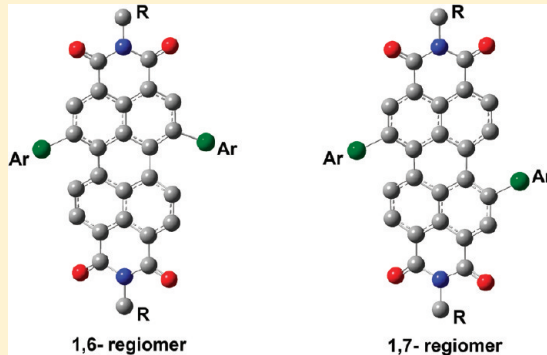
Regioisomers of Perylenediimide: Synthesis, Photophysical, and Electrochemical Properties

Ashok Keerthi and Suresh Valiyaveettill*

Department of Chemistry, National University of Singapore, 3 Science Drive 3, Singapore 117543, Singapore, and NanoCore-NUSNNI, T-Lab Building, National University of Singapore, 5A Engineering Drive 1, Singapore 117411, Singapore

 Supporting Information

ABSTRACT: A series of conjugation extended donor–acceptor 1,6- and 1,7-regiomers of perylenediimide were synthesized, separated, and characterized. The photophysical, electrochemical, and thermal properties of these compounds were investigated and compared. The absorption spectra of 1,6-substituted PDI showed blue shift as compared to its 1,7-substituted PDI. At the same time, the emission spectrum showed no significant differences among the regiomers. Both 1,6- and 1,7-regiomers were thermally stable up to 450 °C and showed different melting and crystallization transitions. The electrochemical studies did not show significant differences in oxidation and redox potentials owing to similar HOMO/LUMO gap of 1,6- and 1,7-regiomers, which is also supported by theoretical calculations. Comparison of properties of a series of 1,6- or 1,7-substituted PDIs showed significant differences. Such regiomERICALLY pure compounds can offer certain advantages in applications, which are currently being investigated.



INTRODUCTION

Perylenediimides (PDIs) are known for their interesting optical and electrical properties and belong to a class of n-type semiconductors due to excellent electron acceptor ability with high molar extinction coefficient, electron mobility, and thermal stability.^{1–4} The bay substitution of PDI is an interesting approach to fine-tune properties^{5–7} and make them processable with common organic solvents. Tremendous scientific interests have been focused on the modification of PDI structures to enhance their optoelectronic and charge transport properties by incorporating substituents.^{7–10} PDI and its derivatives have been extensively utilized for a wide range of applications such as organic and polymeric light emitting devices (OLEDs and PLEDs),^{11–17} laser dyes,^{18,19} organic solar cells,^{20–23} optical switches,²⁴ organic field effect transistors (OFETs),^{25,26} logic gates,²⁷ photosensitizers,²⁸ sensors,^{29,30} biological applications,^{31,32} light-harvesting arrays, and artificial photosynthetic systems.^{33–38} Apart from their diverse and interesting properties, the relatively facile and reversible reduction of PDIs plays a key role in many applications. These facile reductions, combined with easily identifiable excited states have led to their extensive use in fundamental research on photoinduced energy and electron transfer processes.^{4,39,40}

Currently, there is significant interest in the development of PDI derivatives with extended conjugation, which are used in field effect transistors and photovoltaic applications.^{41,42} Substitution and functionalization at the bay region (1-, 6-, 7-, and 12-positions) help to fine-tune the properties of PDIs (Figure 1).^{10,43} More recently, functionalization at the ortho region (2-, 5-, 8-, and 11-positions) of PDI modifies the properties of the

perylene core.^{44–47} Many research groups are working to develop advanced materials with extended conjugation via bay substitution of perylene oligomers and polymers for various applications.^{2,8,48} However, dibromo PDI is the starting material for the synthesis of all these derivatives. Bromination of perylenetetracarboxylic acid dianhydride (PDA) gave dibrominated PDA, which was subsequently converted to dibromo PDI.⁴⁹ The latter was confirmed as a mixture of both 1,6- and 1,7-dibromo PDI in 2004.⁵⁰ However, there is no report on separation of 1,6-dibromo PDI in pure form, although Würthner's method of recrystallization can remove the 1,6-regiomeric to get 1,7-dibromo PDI. Thereafter, separation of piperidinyl and pyrrolidinyl substituted 1,6- and 1,7-regiomers of PDI were reported, which showed different optical and electrochemical properties, but phenoxy substituted 1,6- and 1,7-regiomers of PDI showed no significant differences in their properties.^{51,52} Still there was an ambiguity on properties of π-extended 1,6- and 1,7-PDI systems, and more recently, one report has published with alkyne substitution at the bay positions, while our article was under preparation.⁵³ Here, we report a simple method to isolate 1,6- and 1,7-regiomers of π-extended PDI derivatives (Figure 2) and compare the properties.

RESULTS AND DISCUSSION

Synthesis and Characterization. Synthesis of brominated perylenetetracarboxylic acid dianhydride was achieved via

Received: November 8, 2011

Revised: March 13, 2012

Published: March 22, 2012

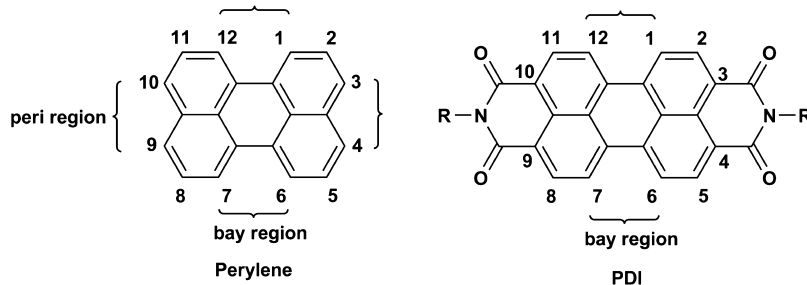


Figure 1. Labeling of position and region in perylene and its derivatives.

iodine-catalyzed bromination of 3,4,9,10-perylenetetracarboxylic acid dianhydride in 98% concentrated sulfuric acid.^{49,50} The crude brominated PDA (Scheme 1) was insoluble in common solvents and subjected to further functionalization without purification. Imidization of the brominated PDA with 2-ethylhexylamine was carried out in *N*-methyl pyrrolidone (NMP) in the presence of acetic acid to produce diimide, which was a mixture of mono-, di-, and tribrominated PDIs.^{7,50,54}

1,6,7-Tribromo PDI (1,6,7-Br₃PDI) and monobromo PDI (Br-PDI) were separated in pure form. The dibromo PDI was obtained as a mixture of 1,6- and 1,7-Br₂PDI regiomers after column chromatography with a ratio of ~1:3, respectively. Suzuki coupling between a regiosomeric mixture of dibromo PDI and various boronic acid pinacol esters gave all compounds in moderate to high yields. Separation of 1,6- and 1,7-regioisomers was achieved via column chromatography using silica gel and a mixture of solvents as eluent. All synthesized compounds were soluble in common organic solvents such as chloroform, dichloromethane, tetrahydrofuran, toluene, and chlorobenzene.

Reaction of 9-[4-(4,4,5,5-tetramethyl-1,3,2-dioxaborolan-2-yl)-phenyl]-9*H*-carbazole⁵⁵ and dibromo PDI gave a mixture of *N,N'*-di(2-ethylhexyl)-1,6-bis[4-(9*H*-carbazol-9-yl)phenyl]perylene-3,4,9,10-tetracarboxydiimide (1,6-CAR) and *N,N'*-di(2-ethylhexyl)-1,7-bis[4-(9*H*-carbazol-9-yl)phenyl]perylene-3,4,9,10-tetracarboxydiimide (1,7-CAR). These 1,6- and 1,7-regiomers were separated on column chromatography using dichloromethane and hexane (1:1) as eluent with 16% and 66% yields, respectively. Peaks on ¹H NMR spectra of both regiomers in the aromatic region were the same, except that two doublets of 1,7-CAR (7.85 and 7.76 ppm) were merged in the case of 1,6-CAR and that the N-CH₂ protons of 1,6-CAR showed two multiplets (at 4.22 and 4.10 ppm). In a similar manner, ¹³C NMR spectra of both regiomers showed similar chemical shifts for carbon atoms on the aromatic ring, but they were significantly different with respect to aliphatic carbons. Compound 1,6-CAR has two sets of peaks for aliphatic carbons with a small difference in chemical shift values (see NMR spectra in Supporting Information).

2-(4-Diphenylaminophenyl)-4,4,5,5-tetramethyl-1,3,2-dioxaborole⁵⁶ was attached to dibromo PDI via Suzuki coupling reaction to give *N,N'*-di(2-ethylhexyl)-1,6-bis(4-diphenylamine)phenylperylene-3,4,9,10-tetracarboxydiimide (1,6-TPA) and *N,N'*-di(2-ethylhexyl)-1,7-bis(4-diphenylamine)phenylperylene-3,4,9,10-tetracarboxydiimide (1,7-TPA). The crude product was purified using column chromatography with a mixture of dichloromethane and hexane (1:1) to give 1,6- and 1,7-TPA with an isolated yield of 18% and 71%, respectively. ¹H NMR spectra of 1,6- and 1,7-TPA were identical, and the only difference was that the aromatic protons were observed at 7.35 ppm with an integration of 12 protons for 1,7-TPA and 8 protons for 1,6-TPA. Another multiplet

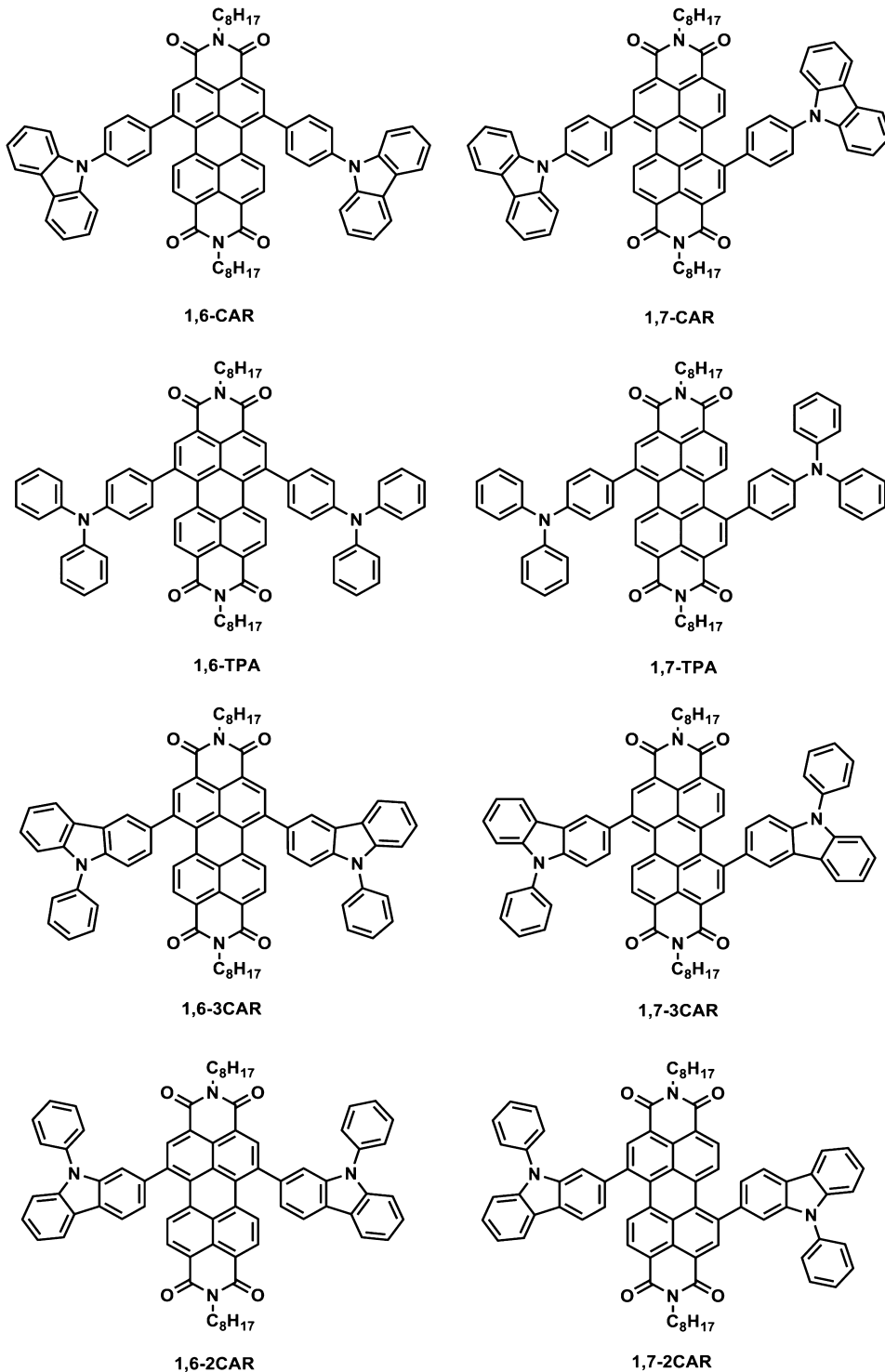
was observed around 7.20 ppm with an integration of 8 protons for 1,7-TPA and 12 protons for 1,6-TPA. A ¹³C NMR spectrum of 1,6-TPA showed two sets of aliphatic carbons as compared to that of the 1,7- regiomer.

The reaction of 9-phenyl-3-(4,4,5,5-tetramethyl-1,3,2-dioxaborolan-2-yl)-9*H*-carbazole⁵⁷ and dibromo PDI yielded a mixture of *N,N'*-di(2-ethylhexyl)-1,6-bis(9-phenyl-9*H*-carbazol-3-yl)perylene-3,4,9,10-tetracarboxydiimide (1,6-3CAR) and *N,N'*-di(2-ethylhexyl)-1,7-bis(9-phenyl-9*H*-carbazol-3-yl)perylene-3,4,9,10-tetracarboxydiimide (1,7-3CAR). In an ¹H NMR spectrum of 1,7-3CAR, the perylene core showed one broad singlet at 8.57 ppm, one broad doublet (8.22 ppm), and one broad N-CH₂ peak (at 4.25 ppm), whereas 1,6-3CAR gave a broad doublet (8.10 ppm) instead of singlet and two broad peaks (around 4.18 and 3.88 ppm) for the N-CH₂ protons. The broadening of peaks may be due to rigidified conformation of bulky 3-carbazole-9*H*-phenyl at the bay positions (see Figure S-6 and S-7, Supporting Information).⁵¹ As expected, ¹³C NMR spectra of both regiomers were different: 1,6-3CAR showed two sets of aliphatic carbon peaks, whereas 1,7-3CAR showed a single set of peaks.

The coupling reaction between 9-phenyl-2-(4,4,5,5-tetramethyl-1,3,2-dioxaborolan-2-yl)-9*H*-carbazole (Scheme 2) and dibromo PDI gave a mixture of *N,N'*-di(2-ethylhexyl)-1,6-bis(9-phenyl-9*H*-carbazol-2-yl)perylene-3,4,9,10-tetracarboxydiimide (1,6-2CAR) and *N,N'*-di(2-ethylhexyl)-1,7-bis(9-phenyl-9*H*-carbazol-2-yl)perylene-3,4,9,10-tetracarboxydiimide (1,7-2CAR), which were separated using silica gel column chromatography using ethyl acetate in hexane (8% v/v) as the mobile phase. ¹H NMR spectra of the two regiosomers showed a similar pattern in the aromatic region and only can be differentiated in the case of the N-CH₂ protons; 1,6-2CAR showed two well-resolved multiplets (around 4.14 and 4.07 ppm). Similarly, the ¹³C NMR spectrum of 1,6-2CAR showed two sets of peaks for aliphatic carbons, and the rest are similar to those of 1,7-2CAR.

In all cases, 1,6-regiomers were found to be different from the corresponding 1,7-regiomers (Scheme 3) in ¹H and ¹³C NMR spectra due to the unsymmetrical nature of the perylene core. Since *R*_f values of regiomers were close, significant attention must be employed for the separation using column chromatography.

Optical and Photophysical Properties. The absorption spectra of all compounds were recorded in chloroform solution (Figure 3), and solid-state absorption studies were done using thin films obtained via drop-casting the solution on quartz plate (Figure 4). The optical band gap was calculated based on the absorption onset. Optical properties such as absorption maxima, molar absorption coefficients, emission maxima, fluorescence lifetime, and optical band gap were presented in Table 1.

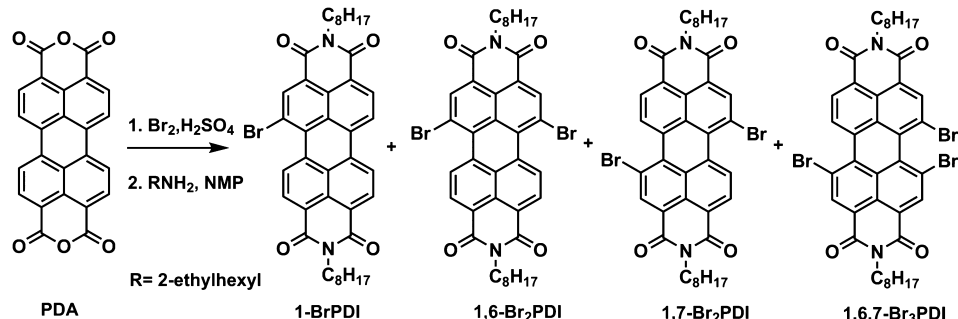
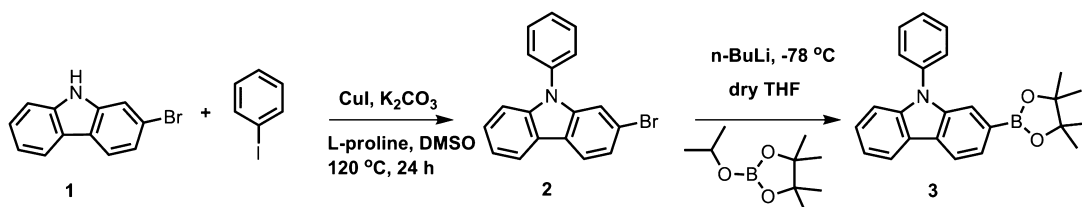
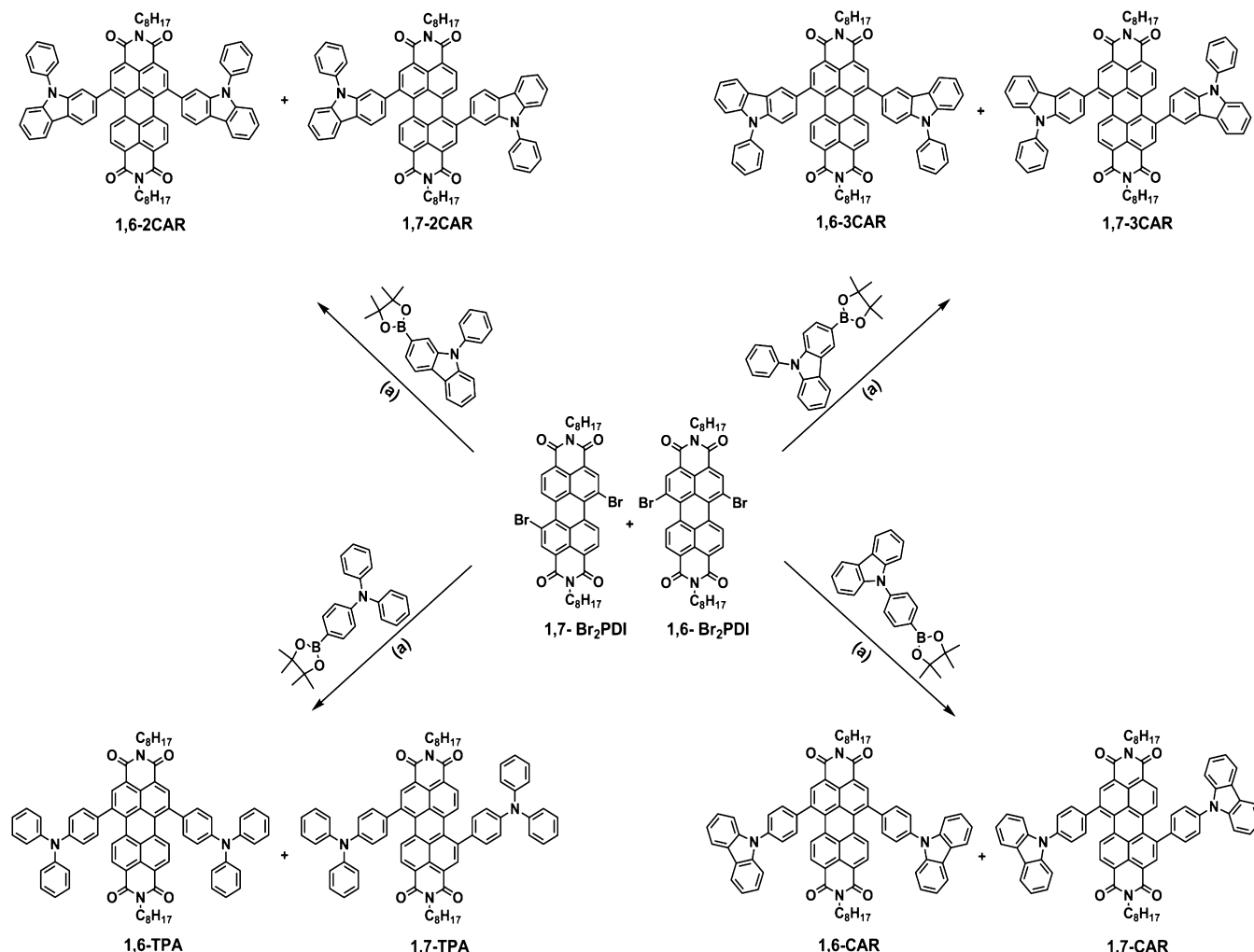
**Figure 2.** Chemical structure of synthesized PDI regiomers.

The PDI derivatives showed absorption maxima at 526 nm, which is attributed to the perylene core $\pi-\pi^*$ transition with characteristic vibronic fine structure.¹⁰

Compound 1,7-CAR showed two absorption maxima at 561 and 523 nm indicating better π -orbital overlapping with the perylene core. This leads to a significant red-shift (35 nm) in the absorption maximum (λ_{\max}) as compared to unsubstituted PDI. Compound 1,6-CAR showed a λ_{\max} at 551 nm, which is 10 nm blue-shifted as compared to 1,7-CAR. An absorption maximum was observed for both compounds at 523 nm, which

indicates a $\pi-\pi^*$ transition from the PDI core. In the solid state, a blue shift was seen from 565 nm (1,7-CAR) to 558 nm (1,6-CAR), whereas a second peak was red-shifted from 507 nm (1,7-CAR) to 522 nm (1,6-CAR). The molar absorption coefficient (ϵ) was found to be higher for 1,7-CAR as compared to 1,6-CAR (Table 1). The calculated optical band gaps of regiomers were more or less similar.

Compounds 1,7- and 1,6-TPA showed two absorption maxima and lower wavelength peak had a high absorption coefficient value. The low energy band was accounted to the charge transfer

Scheme 1. Bromination and Diimidization of Perylenetetracarboxylic Acid Dianhydride (PDA)**Scheme 2.** Synthesis of Compound 3**Scheme 3.** Synthesis of 1,6- and 1,7-Substituted PDIs; (a) 2 M K_2CO_3 , THF, $\text{Pd}(\text{PPh}_3)_4$, 24 h

absorption involving the electronic transition from the triphenylamine to the electron-deficient perylene core, and the high energy

band was assigned to the perylene $\pi-\pi^*$ transition of characteristic vibronic coupling pattern.⁵⁸ In the case of 1,7-TPA, a low energy

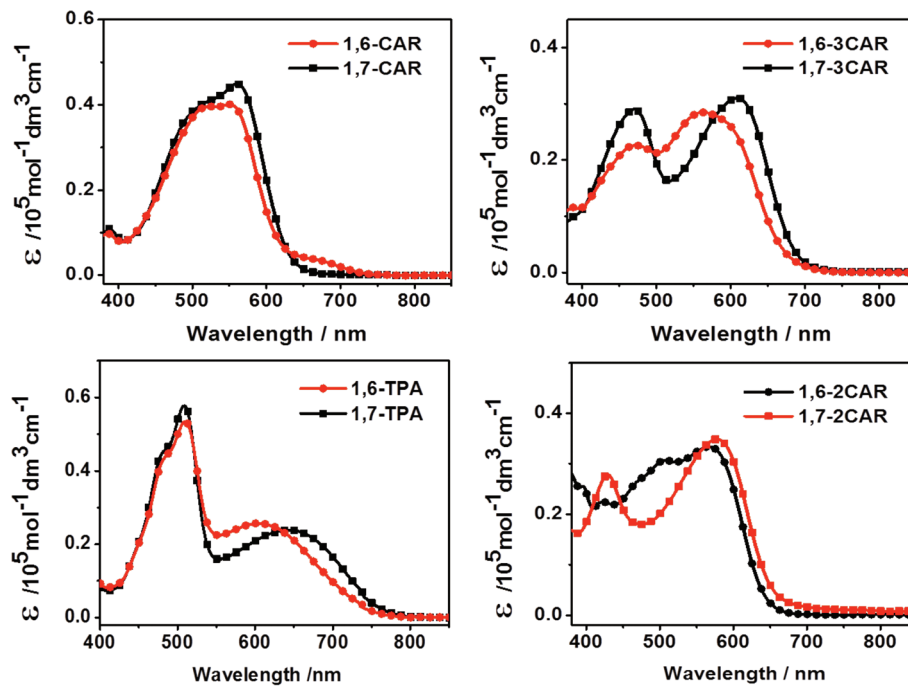


Figure 3. Absorption spectra of the regiomers in chloroform solution at room temperature.

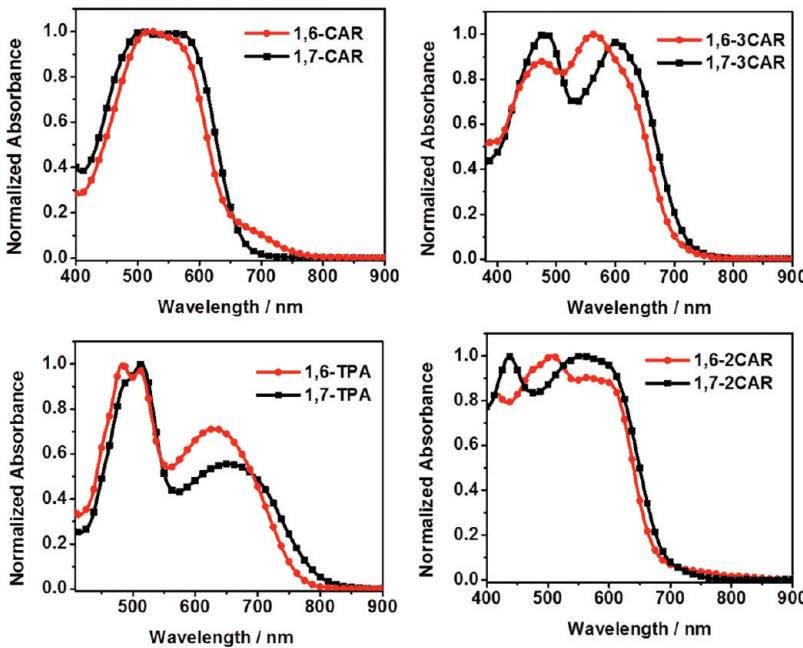


Figure 4. Solid-state absorption spectra of drop casted films on quartz plate at room temperature.

band at 645 nm was red-shifted as compared to 1,6-TPA (606 nm). The second high energy peak was unchanged at 510 nm for both regiomers, which confirms that the high energy absorption band was originated from the perylene moiety. Even though there were significant differences in the absorption maxima, similar optical band gaps were observed for 1,6- and 1,7-TPA compounds.

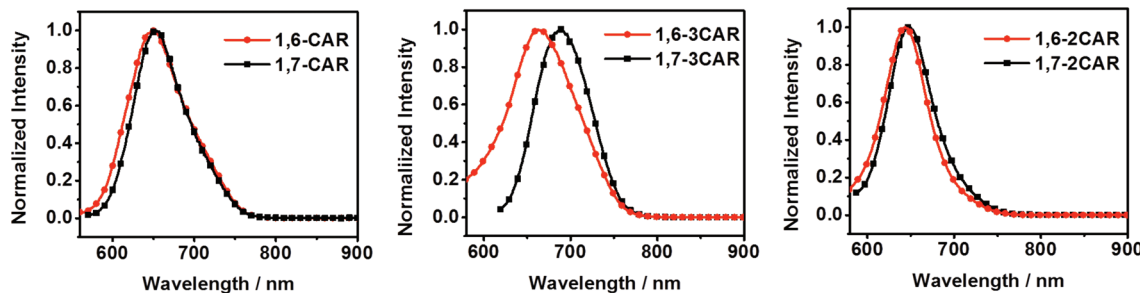
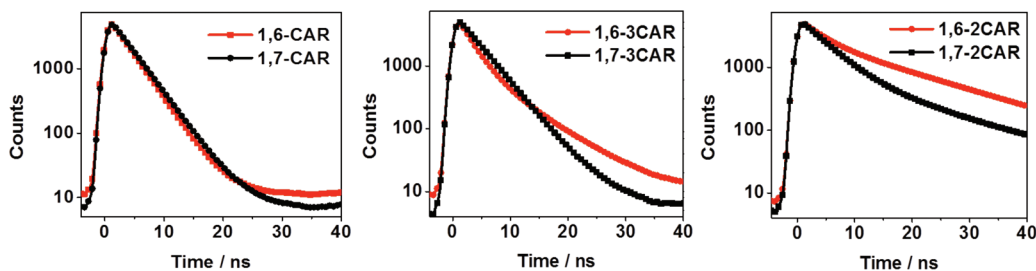
The solution state λ_{\max} of 1,6-3CAR was blue-shifted by 46 nm from that of 1,7-3CAR (609 nm). Here, the second λ_{\max} was found to be same for both regiomers at 472 nm, which is originated from PDI core, and an ϵ value of 1,6-3CAR was low in comparison to that of 1,7-3CAR. The same trend was also

observed in the solid-state absorption spectra, where the absorption maximum for 1,7-3CAR was red-shifted as compared to that of the 1,6-3CAR regiomeric. There was no significant difference in the optical band gap values observed for both 1,6- and 1,7-3CAR compounds.

The absorption spectrum of 1,7-2CAR showed a λ_{\max} of 577 nm at the low energy region, whereas λ_{\max} for 1,6-2CAR appeared at 567 nm. The second absorption peak for 1,6-2CAR at 507 nm was red-shifted as compared to that of 1,7-2CAR. The molar absorption coefficient (ϵ) of 1,7-2CAR was found to be higher than that of 1,6-2CAR. The optical band gap values were similar for both 1,6-2CAR and 1,7-2CAR regiomers.

Table 1. Optical Properties of PDI Regiomers

cmpd	absorption maxima (nm) in chloroform	molar abs. coefficient (10^4 mol $^{-1}$ ·dm 3 ·m $^{-1}$)	absorption maxima in solid state (nm)	emission maxima in chloroform (nm)	fluorescence lifetime τ (ns)	optical band gap (eV)
1,6-CAR	551	4.010	558	651	3.3	1.85
	523	3.961				
1,7-CAR	561	4.494	565	651	3.4	1.87
	523	4.100				
1,6-TPA	606	2.569	632	652	1.61	1.59
	510	5.346				
1,7-TPA	645	2.384	512	652	1.59	1.61
	510	5.774				
1,6-3CAR	563	2.849	562	663	4.1	1.76
	472	2.263				
1,7-3CAR	609	3.104	604	689	3.9	1.74
	472	2.905				
1,6-2CAR	567	3.335	564	644	13.2	1.87
	507	3.064				
1,7-2CAR	577	3.485	557	647	8.8	1.84
	429	2.781				

**Figure 5.** Emission spectra of the regiomers in chloroform solution at room temperature.**Figure 6.** Fluorescence decays of regiomers in chloroform solution.

Compound 1,7-TPA showed broad absorption up to 800 nm, whereas the analogous compound 1,7-CAR showed narrow absorption (up to 680 nm), which was due to electron donating and charge transfer properties of the triphenylamine group. The same trend was observed in the case of 1,6-TPA and 1,6-CAR. The compound 1,7-3CAR (Figure 2, carbazole moiety is linked through position 3) showed significant red shift as compared to the compound 1,7-2CAR (carbazole moiety is linked through position 2), which is expected due to a high resonance effect from the carbazole functionalized at position 3. To our surprise, 1,6-3CAR and 1,6-2CAR had no significant differences in absorption maxima.

Steady-State Emission Properties and Fluorescence Decay. The emission spectra were recorded in chloroform for all molecules using the higher absorption wavelength (λ_{max}) values as excitation wavelength (Figure 5). The emission spectra of both 1,7-CAR and 1,6-CAR showed λ_{emis} at 651 nm with a Stokes shift of 100 nm. The compound 1,7-3CAR showed emission

maximum at 689 nm with a Stokes shift of 80 nm, whereas 1,6-3CAR showed a Stokes shift of 100 nm. In the case of 1,7- and 1,6-2CAR, there was no significant difference in emission spectra with λ_{emis} around 646 nm. As expected, carbazole-substituted PDIs showed weak fluorescence intensity as compared to unsubstituted PDI, and no fluorescence was observed for triphenylamine-substituted PDI regiomers.^{43,58} In comparison to 1,7-2CAR, the emission maximum of 1,7-3CAR was red-shifted by 42 nm, whereas 1,7-CAR showed no significant difference. A similar trend was observed in 1,6-regiomers.

Furthermore, the fluorescence lifetimes of 1,6- and 1,7-regiomers were measured at an excitation wavelength of 560 nm (pulse width of 250 ps) and probing emission maximum of respective regiomers in chloroform solution (Figure 6). The compounds 1,6- and 1,7-CAR showed similar decay profiles, while 1,6-2CAR and 1,7-2CAR showed different fluorescence lifetimes. This may be due to the difference in lifetime of charge separated states of the excited molecules.

In comparison, compound 1,7-CAR and 1,7-3CAR showed insignificant differences in fluorescence lifetime, whereas 1,7-2CAR showed higher fluorescence lifetime (Table 1). The same trend was observed in the case of 1,6-regiomers. It is understood that the substitution of the carbazole moiety linked through position 3 to PDI enhances the charge transfer to the PDI core as compared to the carbazole linked through position 2 to PDI.

Electrochemical Properties. Cyclic voltamograms (CV) of all compounds were recorded in 0.1 M tetrabutylammonium hexafluorophosphate solution of dichloromethane using a standard calomel electrode (SCE) as the reference electrode at 100 mV/s scan rate (Figure 7). CV of all compounds were calibrated with

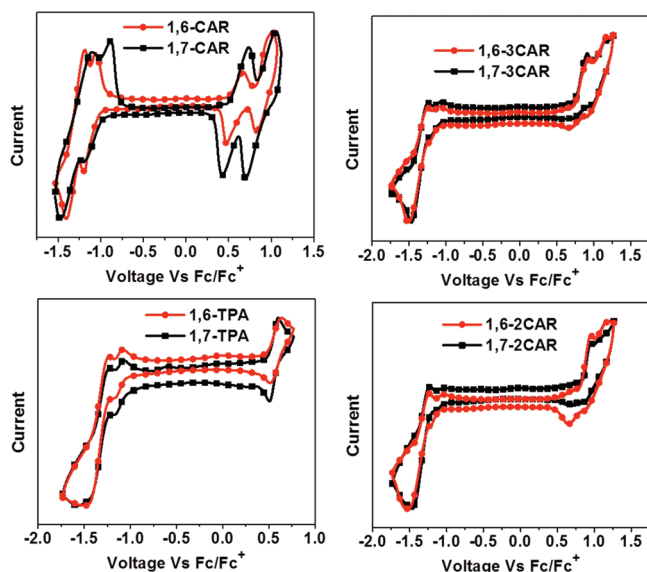


Figure 7. Cyclicvoltammograms of regiomers in dichloromethane containing 0.1 M $t\text{-Bu}_4\text{NPF}_6$ at the scan rate of 100 mV/s.

ferrocene/ferrocenium ion (Fc/Fc^+) redox couple as the internal standard. The oxidation and reduction potentials, and HOMO and LUMO levels, were depicted in Table 2. All compounds showed

Table 2. Electrochemical Properties of PDI Regiomers

cmpd	oxi-1 (V)	oxi-2 (V)	red-1 (V)	red-2 (V)	HOMO ^a (eV)	LUMO ^b (eV)	Eg (eV)
1,6-CAR	0.57	0.92	-1.13	-1.30	-5.31	-3.80	1.51
1,7-CAR	0.58	0.88	-1.04	-1.29	-5.30	-3.82	1.48
1,6-TPA	0.58		-1.12	-1.35	-5.26	-3.78	1.48
1,7-TPA	0.56		-1.12	-1.38	-5.27	-3.81	1.46
1,6-3CAR	0.80	1.04	-1.15	-1.38	-5.40	-3.70	1.70
1,7-3CAR	0.81	1.07	-1.13	-1.36	-5.41	-3.73	1.68
1,6-2CAR	0.80	1.02	-1.12	-1.38	-5.40	-3.70	1.70
1,7-2CAR	0.82	0.98	-1.09	-1.34	-5.43	-3.75	1.68

^aCalculated using the relationship $E_{\text{HOMO}} = -(E_{\text{onset}} + 4.8)$.

^bCalculated using the relationship $E_{\text{LUMO}} = -(E_{\text{red}} + 4.8)$.

two prominent one-electron reduction peaks. The first reduction peak for compound 1,6-CAR (at -1.13 V) was lower by 90 mV to that of 1,7-CAR, whereas the second reduction peak was similar for both 1,6- and 1,7-CAR compounds. No significant difference was found in the first oxidation potential of both regiomers, while the second oxidation potential for 1,6-CAR (0.92 V) was higher than that of 1,7-CAR

(0.88 V). However, the HOMO and LUMO levels were found to be similar for both 1,6- and 1,7-CAR. A small difference in electrochemical band gap for both regiomers was observed.

Similarly, compounds 1,7- and 1,6-TPA showed similar one-electron reduction potentials. A small difference (30 mV) in the second one-electron reduction potentials of regiomers was observed. Compound 1,6-TPA showed the first oxidation potential at 0.58 V, which was 20 mV higher than that of 1,7-TPA. Interestingly, both regiomers did not show a second oxidation peak within the potential window of electrolyte. The HOMO–LUMO gap was found to be similar for both regiomers.

The first reduction peak for compound 1,6-3CAR (-1.15 V) was 20 mV lower than that of 1,7-3CAR. The second reduction peak of 1,6-3CAR (-1.38 V) was shifted negatively by 20 mV as compared to 1,7-3CAR. However, the first oxidation peak was found to be similar for 1,6-3CAR (0.80 V) and 1,7-3CAR (0.81 V), and the second oxidation of 1,6-3CAR was 30 mV lower than that of 1,7-3CAR (1.07 V). The HOMO and LUMO levels for both 1,6- and 1,7-3CAR were found to be similar, which indicated no significant differences for both regiomers in the energy levels.

The first one electron reduction of 1,7-2CAR (-1.09 V) was observed to be 30 mV higher than corresponding the 1,6-regiomer, and the second one electron reduction value of 1,6-2CAR was 40 mV lower than that of 1,7-2CAR (-1.34 V). The first one electron loss for 1,7-2CAR (0.82 V) was 20 mV higher than that of 1,6-2CAR, and the second one electron loss was 40 mV more than that of 1,6-2CAR (0.98 V). The HOMO levels for 1,6- and 1,7-2CAR were similar, but the LUMO levels were slightly different (Table 2). Surprisingly, the compounds with carbazole linked through 2 and 3 positions to PDI showed similar electrochemical properties, even though they exhibited considerable differences in optical properties.

The HOMO and LUMO energy level values for 1,7-CAR and 1,7-TPA were found to be similar, and an analogous trend was also observed for 1,6-CAR and 1,6-TPA. Both compounds, 1,7-3CAR and 1,7-2CAR showed similar oxidation and reduction potentials with the same electrochemical band gap. A similar trend was observed in the case of 1,6-3CAR and 1,6-2CAR. The first reduction potentials of regiomers were generated from reduction of the perylene core and gave rise to the LUMO energy level.

Thermal Properties. Thermogravimetric analyses (TGA) and differential scanning calorimetry (DSC) studies were carried out under nitrogen atmosphere. TGA studies revealed that all compounds were stable up to 450 °C (see Figure S-1, Supporting Information). However, DSC traces were found to be different for both regiomers. Compound 1,7-CAR showed a glass transition temperature (T_g) at 169 °C and a crystallization temperature (T_{cryst}) at 226 °C, but 1,6-CAR did not show T_g or T_{cryst} . Compound 1,6-TPA showed a very sharp melting peak at 250 °C with no glass transition temperature or crystallization peak, whereas 1,7-TPA showed a melting point (T_m) at 233 °C (Figure 8).

In the case of 1,6-3CAR, T_g was observed at 150 °C with no crystallization peak (T_{cryst}), whereas the T_g and T_{cryst} of 1,7-3CAR were observed at 191 and 294 °C, respectively. Compound 1,7-3CAR melted at 319 °C, but the corresponding 1,6-regiomeric did not show a sharp melting peak. Compound 1,7-2CAR showed slightly higher T_m , T_g and T_{cryst} in contrast to the 1,6-regiomeric (Table 3).

Thermal studies revealed that 1,6-regiomers showed higher melting points as compared to 1,7-regiomers. The compound

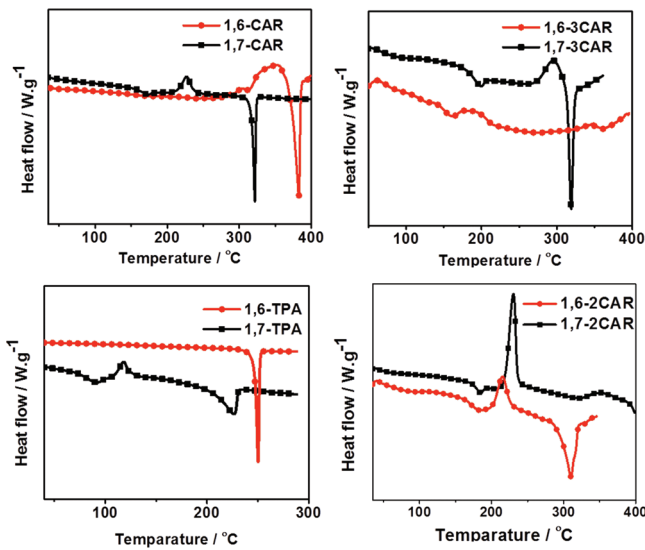


Figure 8. DSC traces of PDI regiomers recorded at a heating rate of $10\text{ }^{\circ}\text{C min}^{-1}$ under nitrogen atmosphere.

Table 3. Thermal Characteristics of PDI Regiomers

cmpd	T (10 wt % loss) ($^{\circ}\text{C}$)	T_d ($^{\circ}\text{C}$)	T_m ($^{\circ}\text{C}$)	T_g ($^{\circ}\text{C}$)	T_{cryst} ($^{\circ}\text{C}$)
1,6-CAR	451	400	382		
1,7-CAR	455	420	322	169	226
1,6-TPA	389	360	250		
1,7-TPA	427	381	233	84	118
1,6-3CAR	458	413	362	150	
1,7-3CAR	432	412	319	191	294
1,6-2CAR	475	418	310	170	215
1,7-2CAR	465	398	321	181	230

1,7-3CAR had higher T_g and T_{cryst} than 1,7-2CAR and 1,7-CAR. For the compound 1,7-TPA, T_{cryst} was observed to be significantly low compared to that of 1,7-CAR. In the case of 1,6-regiomers, T_{cryst} was not observed except for in 1,6-2CAR.

Theoretical Calculations. The Gaussian calculations were carried out on Gaussian09 at the density functional theory (DFT) level with the B3LYP function using 6-31G* as a basis set. The geometry optimized structures (see Supporting Information) and frontier orbital energy levels were calculated. The twisting angle (α) between two naphthalene units of the substituted perylene core was calculated (Figure 9), and all results were depicted in Table 4. The twist angles (α) of bromo-substituted PDI were 22.6° and 22.1° for both regiomers 1,6- and 1,7-Br₂PDI, respectively, which was close to the previously reported angle 21.0° for 1,7-Br₂PDI.⁶ The HOMO energy levels of both regiomers were the same (at -6.12 eV), and the LUMO energy levels were slightly different for 1,6- and 1,7-Br₂PDI. As a result, the HOMO–LUMO gap was almost the same for 1,6- and 1,7-Br₂PDI.

The calculated HOMO and LUMO levels for both 1,6- and 1,7-CAR were at -5.47 and -3.43 eV . In the case of 1,6- and 1,7-2CAR, the LUMO level exists at -3.18 eV , whereas the HOMO level was located at -5.47 and -5.44 eV , respectively. There was no difference in LUMO energy levels of both 1,6- and 1,7-3CAR; however, the HOMO energy levels were at -5.36 and -5.33 eV , with a small difference. The twist angle (α) values were at 20.7° and 20.2° for both 1,6- and 1,7-3CAR,

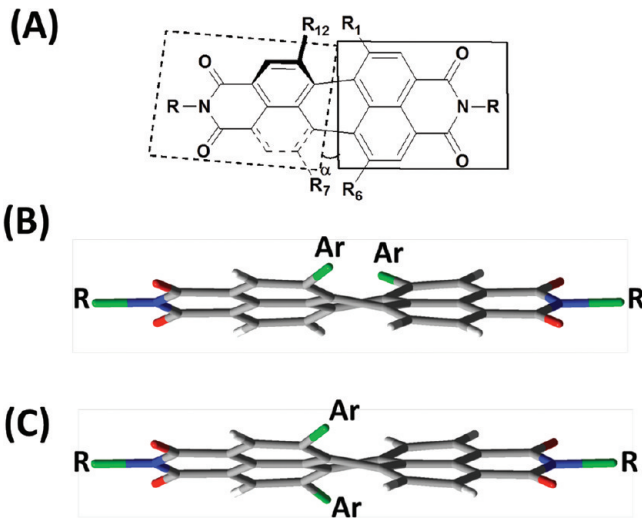


Figure 9. Schematic view of twisting angle of (A) bay-substituted, (B) 1,7-substituted, and (C) 1,6-substituted PDIs.

Table 4. Theoretical Calculations of PDI Regiomers

cmpd	av α (Θ)	HOMO (eV)	LUMO (eV)	band gap (eV)
1,6-Br ₂ PDI	22.58	-6.12	-3.59	2.53
1,7-Br ₂ PDI	22.14	-6.12	-3.57	2.55
1,6-CAR	20.47	-5.47	-3.43	2.04
1,7-CAR	20.09	-5.47	-3.43	2.04
1,6-TPA	20.79	-5.09	-3.18	1.91
1,7-TPA	20.27	-5.09	-3.18	1.91
1,6-3CAR	20.70	-5.36	-3.13	2.23
1,7-3CAR	20.20	-5.33	-3.13	2.20
1,6-2CAR	20.03	-5.47	-3.18	2.29
1,7-2CAR	19.55	-5.44	-3.18	2.26

respectively. No significant difference in HOMO and LUMO energy levels was observed for both 1,6- and 1,7-TPA. In the case of carbazole linked through the second position (1,6- and 1,7-2CAR) and third position (1,6- and 1,7-3CAR) to PDI, the HOMO orbitals were evenly distributed on carbazole as well as the perylene core, while the LUMO orbitals were located on the PDI core (Figure 10). In the case of phenylene-bridged carbazole (1,6- and 1,7-CAR) and triphenylamine-substituted PDIs (1,6- and 1,7-TPA), the HOMO was mostly localized on the phenyl carbazole and triphenylamine, and the LUMO was fully localized on the PDI core. The twist angle (α) for 1,6-regiomers was always higher than the corresponding 1,7-regiomers, which indicates that two substitutions on the same naphthalene unit of PDI causes more twisting of the molecule.

EXPERIMENTAL METHODS

General Considerations. Materials. All chemicals and reagents were purchased from commercial suppliers and used without further purification. Solvents used for spectroscopic measurements were spectral grade quality. Tetrahydrofuran (THF) was distilled in the presence of metallic sodium. The compounds 9-phenyl-3-(4,4,5,5-tetramethyl-1,3,2-dioxaborolan-2-yl)-9H-carbazole,⁵⁷ 9-[4-(4,4,5,5-tetramethyl-1,3,2-dioxaborolan-2-yl)phenyl]-9H-carbazole,⁵⁸ 2-bromo-9H-carbazole,⁵⁹ and 2-(4-diphenylaminophenyl)-4,4,5,5-tetramethyl-1,3,2-dioxaborolane⁵⁶ were synthesized by following literature reports. All reactions were monitored by thin-layer chromatography (TLC) on silica

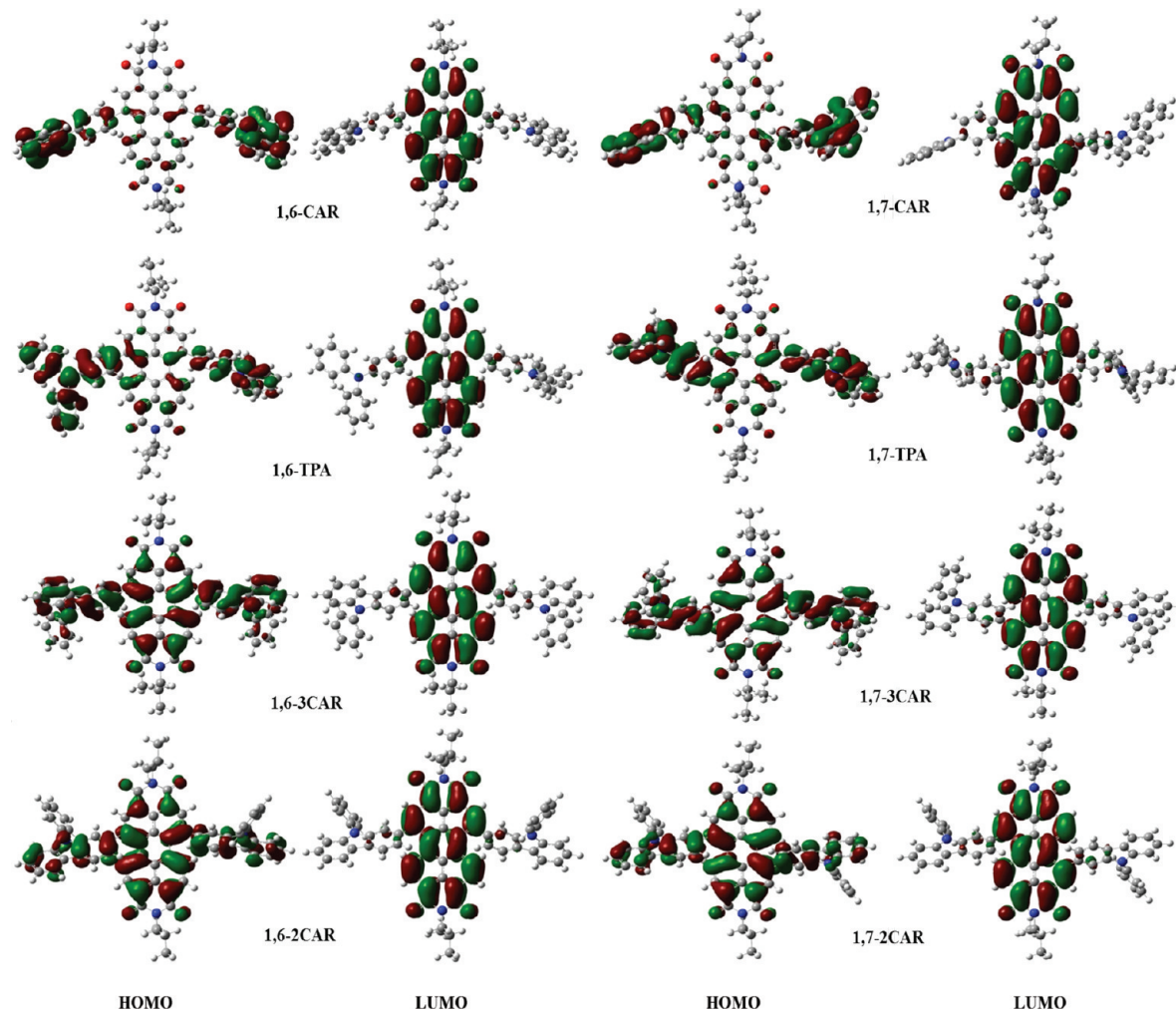


Figure 10. Frontier orbitals of PDI regiomers calculated using density functional theory (DFT) at the B3LYP/6-31G (d) level.

gel plates. Preparative separations were performed by column chromatography on silica gel grade 60 (0.040–0.063 mm).

Instrumentation and Characterization. ^1H NMR spectra were recorded on a Bruker ACF300 (300 MHz) spectrometer. The chemical shifts were reported in ppm and referenced to the residual solvent peak: s = singlet, d = doublet, t = triplet, m = multiplet, and b = broad. FAB-mass spectra were obtained on a Finnigan MAT95XL-T and Micromass VG7035 mass spectrometer. Elemental analysis was carried out on Elementar Vario Micro Cube. The UV-vis and emission spectra were measured on a UV-1601PC Shimadzu spectrophotometer and RF-5301PC Shimadzu spectrofluorophotometer. Fluorescence lifetimes were measured by using TCSPC (Horiba Jobin Yvon IBH ltd) by exciting with NanoLED of wavelength 560 nm (pulse width of 250 ps). Thermal data were recorded under nitrogen atmosphere on a TA Instruments Q100.

A cyclic voltammogram was recorded with a computer controlled CHI electrochemical analyzer at a constant scan rate of 100 mV/s. Measurements were performed in an electrolyte solution of 0.1 M tetrabutylammonium hexafluorophosphate dissolved in degassed dichloromethane. The electrochemical cell consists of three electrode systems with a platinum disk as the working electrode, platinum rod as the counter electrode, and a standard calomel electrode (SCE) as the reference electrode. The potentials were calibrated using ferrocene as the internal standard. The onset of oxidation ($E_{\text{ox}}^{\text{onset}}$) and reduction

($E_{\text{red}}^{\text{onset}}$) were used to calculate HOMO and LUMO energy levels using the relationship $E_{\text{HOMO}} = -(4.8 + E_{\text{ox}}^{\text{onset}})$ and $E_{\text{LUMO}} = -(4.8 + E_{\text{red}}^{\text{onset}})$, respectively. Geometry optimizations were performed in Gaussian09⁶⁰ at the density functional theory (DFT) level with the B3LYP functional and a 6-31G* basis set. The HOMO and LUMO surfaces were generated from the optimized geometries using Gaussview 5.⁶¹

9-(Phenyl)-2-bromo-9H-carbazole (2). A mixture of 2-bromo-9H-carbazole (1) (5.0 g, 20.3 mmol), 4-iodobenzene (4.5 g, 22.1 mmol), and K_2CO_3 (4.16 g, 30 mmol) in DMSO (70 mL) was stirred under N_2 for 30 min (Scheme 3). Followed by the addition of CuI (0.40 g, 2.1 mmol) and L-proline (0.48 g, 4.2 mmol), the mixture was refluxed at 120 °C under nitrogen for 24 h. After cooling to room temperature, the reaction mixture was poured into water, and the product was extracted using diethyl ether. The crude product was purified by column chromatography using hexane as the eluent to give a white product (4.57 g, 70% yield). ^1H NMR (300 MHz, CDCl_3 , δ ppm): 8.11 (d, J = 7.80 Hz, 1H), 7.99 (d, J = 8.40 Hz, 1H), 7.65–7.60 (m, 2H), 7.55–7.52 (m, 4H), 7.43–7.37 (m, 3H), 7.32–7.30 (m, 1H). ^{13}C NMR (75 MHz, CDCl_3 , δ ppm): 141.7, 141.1, 137.0, 130.0, 127.8, 127.1, 126.3, 123.0, 122.8, 122.2, 121.4, 120.3, 120.2, 119.4, 112.7, 109.9. MS (EI) m/z : 321.1. Anal. Calcd for $\text{C}_{18}\text{H}_{12}\text{BrN}$: C, 67.10; H, 3.75; N, 4.35; Br, 24.80. Found: C, 67.16; H, 3.70; N, 4.27; Br, 24.91.

9-(Phenyl)-2-(4,4,5,5-tetramethyl-1,3,2-dioxaborolan-2-yl)-9H-carbazole (3). N-Butyl lithium (2 M solution in cyclohexane) (2.5 mL, 5 mmol) was added slowly to compound 2 (1.28 g, 4 mmol) in dried THF solution at -78 °C and stirred for 20 min. To this mixture, 2-isopropoxy-4,4,5,5-tetramethyl-[1,3,2] dioxaborolane (1.0 g, 5.4 mmol) was added slowly and stirred for 2 h at -78 °C and then stirred overnight at room temperature (Scheme 2). The reaction mixture was quenched with water and extracted with diethyl ether. The crude product was purified by column chromatography using 5% ethyl acetate in hexane to give a white solid (0.83 g, 56% yield). ¹H NMR (300 MHz, CDCl₃, δ ppm): 8.18–8.14 (m, 2H), 7.84 (s, 1H), 7.76 (d, J = 7.80 Hz, 1H), 7.65–7.60 (m, 4H), 7.59–7.56 (m, 1H), 7.51–7.36 (m, 2H), 7.31–7.28 (m, 1H), 1.36 (m, 12H). ¹³C NMR (75 MHz, CDCl₃, δ ppm): 141.5, 140.5, 137.7, 129.9, 127.5, 127.4, 126.1, 125.8, 124.2, 123.1, 120.8, 119.8, 119.5, 116.0, 109.9, 83.7, 24.9. MS (EI) m/z: 369.2. Anal. Calcd for C₂₄H₂₄BNO₂: C, 78.06; H, 6.55; N, 3.79. Found: C, 78.16; H, 6.61; N, 3.69.

Bromination and Imidization of Perylenetetracarboxylic acid Dianhydride.^{7,49,50,54} Perylene tetracarboxylic acid anhydride (10.0 g, 25.4 mmol) was dispersed in conc. H₂SO₄ (150 mL) with a catalytic amount of I₂ (25 mg). To the reaction mixture, bromine (9.4 g, 58.5 mmol) was added slowly within a period of 0.5 h and stirred at 85 °C for 24 h (Scheme 1). The reaction mixture was cooled to room temperature and slowly poured into water (1 L). The precipitate was filtered, washed with water and methanol, and dried in vacuum. This crude brominated perylenetetracarboxylic acid dianhydride (Br-PDA) was directly used for the imidization reaction. The crude Br-PDI (5.5 g, 10 mmol) was dispersed in 100 mL of N-methyl pyrrolidone (NMP), and to this, 2-ethylhexylamine (2 g, 23.0 mmol) and acetic acid (5.0 mL) were added in nitrogen atmosphere. The reaction mixture was stirred for 24 h at 90 °C. After cooling to room temperature, the mixture was poured into water and filtered. The precipitate was washed with water, methanol, and purified by column chromatography on silica gel using chloroform and hexane (2:1) mixture as eluent. At first elution, 1,6,7-tribromo-N,N'-di(2-ethylhexyl)-perylene-3,4,9,10-tetracarboxydiimide (1,6,7-Br₃PDI) (0.054 g, 0.7% yield) was obtained as a minor product, the mixture of 1,6- and 1,7-dibromo-N,N'-di(2-ethylhexyl)-perylene-3,4,9,10-tetracarboxydiimide (5.5 g, 71% yield) was obtained during the second elution, and 1-bromo-N,N'-di(2-ethylhexyl)-perylene-3,4,9,10-tetracarboxydiimide (Br-PDI) (0.10 g, 1% yield) was obtained on the third elution as a minor product.

General Condition for Suzuki Coupling Reaction. To a 100 mL two-neck round-bottom flask under nitrogen atmosphere, the dibromo PDI (0.386 g, 0.5 mmol) and respective boronic acid pinacol ester (1.2 mmol) were dissolved in 20 mL of tetrahydrofuran (THF). To this reaction mixture, 10 mL of prepurged 2 M K₂CO₃ aqueous solution and catalyst Pd(PPh₃)₄ (0.058 g, 0.05 mmol) were added and stirred for 24 h at 80 °C under nitrogen atmosphere (Scheme 3). The reaction mixture was allowed cool to room temperature and was extracted with dichloromethane. The collected organic layers were dried over anhydrous sodium sulfate. The solvent was removed under reduced pressure. The crude product was purified by silica gel column chromatography (see details below).

N,N'-Di(2-ethylhexyl)-1,6-bis(4-diphenylamine)-phenylperylene-3,4,9,10-tetracarboxydiimide (1,6-TPA). The crude compound was purified by column chromatography using 1:1 hexane and dichloromethane as the eluent. The

retention factor (*R*_f) of 1,6-TPA and 1,7-TPA are 0.54 and 0.44, respectively. The amount of 1,6-TPA obtained was 0.085 g (18%). ¹H NMR (300 MHz, CDCl₃, δ ppm): 8.61 (s, 2H, Per-H), 8.25 (d, J = 8.40, 2H, Per-H), 8.02 (d, J = 8.40, 2H, Per-H), 7.36–7.27 (m, 8H), 7.24–7.18 (m, 12H), 7.14–7.07 (m, 8H), 4.19–4.14 (m, 2H, N-CH₂), 4.10–4.06 (m, 2H, N-CH₂), 1.96–1.92 (m, 2H), 1.42–1.31 (m, 16H), 0.96–0.87 (m, 12H). ¹³C NMR (75 MHz, CDCl₃, δ ppm): 163.97, 163.96, 148.4, 147.2, 142.0, 135.6, 135.2, 134.8, 132.6, 129.8, 129.6, 129.5, 129.3, 128.4, 126.8, 125.0, 123.9, 123.6, 122.2, 121.8, 44.2, 38.0, 30.8, 30.7, 28.8, 28.7, 24.1, 24.01, 23.1, 23.1, 14.1, 10.7, 10.6. FAB-MASS (+VE): (m/z) 1101.527. Anal. Calcd for C₇₆H₆₈N₄O₄: C, 82.88; H, 6.22; N, 5.09. Found: C, 82.56; H, 6.30; N, 4.97.

N,N'-Di(2-ethylhexyl)-1,7-bis[(4-diphenylamine)phenyl]-perylene-3,4,9,10-tetracarboxydiimide (1,7-TPA). The amount of 1,7-TPA obtained was 0.385 g (71%). ¹H NMR (300 MHz, CDCl₃, δ ppm): 8.61 (s, 2H, Per-H), 8.23 (d, J = 9.00, 2H, Per-H), 8.04 (d, J = 9.00, 2H, Per-H), 7.40–7.31 (m, 12H), 7.21–7.18 (m, 8H), 7.15–7.07 (m, 8H), 4.18–4.09 (m, 4H, N-CH₂), 1.97–1.93 (m, 2H), 1.41–1.31 (m, 16H), 0.96–0.87 (m, 12H). ¹³C NMR (75 MHz, CDCl₃, δ ppm): 163.9, 148.5, 147.2, 140.8, 135.4, 135.2, 135.1, 132.3, 129.9, 129.6, 129.5, 129.3, 129.1, 127.5, 125.1, 123.8, 123.7, 122.1, 121.7, 44.2, 38.0, 30.8, 28.7, 24.1, 23.1, 14.1, 10.6. FAB-MASS: (m/z) 1101.527. Anal. Calcd for C₇₆H₆₈N₄O₄: C, 82.88; H, 6.22; N, 5.09. Found: C, 82.79; H, 6.19; N, 4.87.

N,N'-Di(2-ethylhexyl)-1,6-bis[4-(9H-carbazol-9-yl)phenyl]-perylene-3,4,9,10-tetracarboxydiimide (1,6-CAR). The crude compound was purified by column chromatography using 1:1 hexane and dichloromethane as the eluent. The *R*_f of 1,6-CAR and 1,7-CAR are 0.33 and 0.26, respectively. The amount of 1,6-CAR obtained was 0.087 g (16%). ¹H NMR (300 MHz, CDCl₃, δ ppm): 8.77 (s, 2H, Per-H), 8.31 (d, J = 9.00, 2H, Per-H), 8.19 (d, J = 6.00, 4H, Car-H), 8.06 (d, J = 9.00, 2H, Per-H), 7.73 (m, 8H, Ph-H), 7.52–7.50 (m, 8H, Car-H), 7.38–7.33 (m, 4H, Car-H), 4.25–4.20 (m, 2H, N-CH₂), 4.13–4.08 (m, 2H, N-CH₂), 2.02 (m, 1H), 1.93 (m, 1H), 1.44–1.31 (m, 16H), 1.01–0.87 (m, 12H). ¹³C NMR (75 MHz, CDCl₃, δ ppm): 163.74, 163.72, 141.5, 141.1, 140.6, 138.2, 135.4, 134.1, 133.1, 130.5, 129.9, 129.7, 129.6, 128.8, 128.7, 128.5, 127.4, 126.3, 123.6, 122.5, 122.4, 120.5, 120.4, 109.6, 44.36, 44.30, 38.05, 37.99, 30.8, 30.7, 28.8, 28.6, 24.1, 24.0, 23.07, 23.06, 14.12, 14.08, 10.7, 10.6. FAB-MASS (-VE): (m/z) 1096.495. Anal. Calcd for C₇₆H₆₄N₄O₄: C, 83.18; H, 5.88; N, 5.11. Found: C, 83.30; H, 6.04; N, 5.10.

N,N'-Di(2-ethylhexyl)-1,7-bis[4-(9H-carbazol-9-yl)phenyl]-perylene-3,4,9,10-tetracarboxydiimide (1,7-CAR). The yield of the compound was 66% (0.359 g). ¹H NMR (300 MHz, CDCl₃, δ ppm): 8.76 (s, 2H, Per-H), 8.33 (d, J = 8.07, 2H, Per-H), 8.19 (d, J = 6.00, 4H, Car-H), 8.09 (d, J = 8.10, 2H, Per-H), 7.85 (d, J = 9.00, 4H, Ph-H), 7.76 (d, J = 9.00, 4H, Ph-H), 7.53–7.51 (m, 8H, Car-H), 7.38–7.33 (m, 4H, Car-H), 4.22–4.13 (m, 4H, N-CH₂), 1.99–1.96 (m, 2H), 1.43–1.33 (m, 16H), 0.98–0.88 (m, 12H). ¹³C NMR (75 MHz, CDCl₃, δ ppm): 163.75, 163.68, 141.1, 140.6, 140.2, 138.3, 135.4, 134.8, 132.6, 130.7, 130.3, 129.6, 129.4, 128.7, 128.0, 126.3, 123.7, 122.6, 122.4, 120.5, 120.4, 109.6, 44.3, 38.0, 30.8, 28.1, 24.1, 23.1, 14.1, 10.7. FAB-MASS (-VE): (m/z) 1096.494. Anal. Calcd for C₇₆H₆₄N₄O₄: C, 83.18; H, 5.88; N, 5.11. Found: C, 82.98; H, 6.07; N, 5.04.

N,N'-Di(2-ethylhexyl)-1,6-bis(9-phenyl-9H-carbazol-3-yl)-perylene-3,4,9,10-tetracarboxydiimide (1,6-3CAR). The crude

compound was purified by column chromatography using 10% ethyl acetate in hexane as the eluent. The R_f of 1,6-3CAR and 1,7-3CAR were 0.67 and 0.75, respectively. The amount of 1,6-3CAR obtained 0.098 g (18%). ^1H NMR (300 MHz, CDCl_3 , δ ppm): 8.73 (d, $J = 20$, 2H, Per-H), 8.38 (b, 1H, Car-H), 8.23 (d, $J = 6.90$, 1H, Per-H), 8.11 (d, $J = 6.75$, 1H, Per-H), 7.97 (b, 2H, Per-H), 7.87–7.80 (m, 3H, Car-H), 7.65 (m, 8H, Car-H), 7.53–7.46 (m, 8H, Car-H), 7.38–7.32 (m, 4H, Car-H), 4.21–4.12 (m, 2H, N-CH₂), 3.96–3.86 (m, 2H, N-CH₂), 2.00 (m, 1H), 1.83 (m, 1H), 1.46–1.29 (m, 16H), 1.01–0.84 (m, 12H). ^{13}C NMR (75 MHz, CDCl_3 , δ ppm): 164.0, 163.8, 142.8, 142.7, 141.4, 140.6, 137.2, 135.9, 134.8, 134.7, 134.2, 134.0, 132.8, 130.0, 129.8, 129.4, 128.9, 128.3, 127.8, 127.2, 126.8, 126.6, 124.9, 123.1, 121.6, 120.8, 120.5, 111.3, 110.2, 44.3, 44.1, 38.9, 37.8, 30.9, 30.7, 29.7, 28.6, 24.2, 24.0, 23.07, 23.03, 14.12, 14.07, 10.7, 10.6. FAB-MASS (+VE): (*m/z*) 1097.495. Anal. Calcd for $\text{C}_{76}\text{H}_{64}\text{N}_4\text{O}_4$: C, 83.18; H, 5.88; N, 5.11. Found: C, 82.99; H, 6.03; N, 4.97.

N,N'-Di(2-ethylhexyl)-1,7-bis(9-phenyl-9H-carbazol-3-yl)-perylene-3,4,9,10-tetracarboxydiimide (1,7-3CAR). The yield of the compound was 65% (0.354 g). ^1H NMR (300 MHz, CDCl_3 , δ ppm): 8.57 (s, 2H, Per-H), 8.51 (s, 2H, Car-H), 8.22 (d, $J = 24.00$, 2H, Per-H), 8.05 (d, $J = 8.02$, 2H, Per-H), 7.62 (b, 10H, Car-H), 7.47 (b, 10H, Car-H), 7.21–7.17 (m, 2H, Car-H), 4.25 (b, 4H, N-CH₂), 1.97 (m, 2H), 1.42–1.30 (m, 16H), 0.98–0.90 (m, 12H). ^{13}C NMR (75 MHz, CDCl_3 , δ ppm): 163.8, 163.5, 141.4, 140.7, 137.2, 135.5, 134.4, 133.6, 131.5, 130.0, 129.7, 128.9, 128.7, 127.7, 127.1, 126.9, 126.6, 125.43, 125.41, 123.42, 123.40, 123.36, 121.8, 121.3, 121.1, 120.7, 110.1, 44.4, 38.0, 30.9, 28.8, 24.2, 23.1, 14.2, 10.7. FAB-MASS (+VE): (*m/z*) 1097.499. Anal. Calcd for $\text{C}_{76}\text{H}_{64}\text{N}_4\text{O}_4$: C, 83.18; H, 5.88; N, 5.11. Found: C, 82.89; H, 5.84; N, 5.00.

N,N'-Di(2-ethylhexyl)-1,6-bis(9-phenyl-9H-carbazol-2-yl)-perylene-3,4,9,10-tetracarboxydiimide (1,6-2CAR). The crude compound was purified by column chromatography using 10% ethyl acetate in hexane as the eluent. The R_f of 1,6-2CAR and 1,7-2CAR were 0.71 and 0.76, respectively. The amount of 1,6-2CAR obtained was 0.077 g (12%). ^1H NMR (300 MHz, CDCl_3 , δ ppm): 8.67 (s, 2H, Per-H), 8.18 (d, $J = 7.2$, 4H, Car-H), 8.05 (d, $J = 8.10$, 2H, Per-H), 7.80 (d, $J = 9.00$, 2H, Per-H), 7.60–7.57 (m, 6H, Car-H), 7.48–7.46 (m, 10H, Car-H), 7.38–7.33 (m, 4H, Car-H), 4.17–4.12 (m, 2H, N-CH₂), 4.09–4.03 (m, 2H, N-CH₂), 1.93 (m, 2H), 1.39–1.30 (m, 16H), 0.96–0.88 (m, 12H). ^{13}C NMR (75 MHz, CDCl_3 , δ ppm): 163.9, 163.7, 142.8, 142.1, 141.7, 140.2, 137.3, 135.5, 134.6, 133.1, 130.0, 129.9, 129.8, 129.5, 128.8, 128.2, 127.7, 127.1, 126.9, 126.6, 123.4, 122.8, 122.1, 122.0, 121.8, 120.8, 120.6, 120.5, 110.0, 109.9, 44.3, 44.2, 38.0, 37.9, 30.8, 30.7, 28.7, 28.6, 24.1, 24.0, 23.1, 23.0, 14.1, 10.6. FAB-MASS (+VE): (*m/z*) 1097.498. Anal. Calcd for $\text{C}_{76}\text{H}_{64}\text{N}_4\text{O}_4$: C, 83.18; H, 5.88; N, 5.11. Found: C, 83.24; H, 5.21; N, 4.96.

N,N'-Di(2-ethylhexyl)-1,7-bis(9-phenyl-9H-carbazol-2-yl)-perylene-3,4,9,10-tetracarboxydiimide (1,7-2CAR). The yield of the compound was 60% (0.385 g). ^1H NMR (300 MHz, CDCl_3 , δ ppm): 8.63 (s, 2H, Per-H), 8.19 (d, $J = 7.5$, 4H, Car-H), 8.01 (d, $J = 8.22$, 2H, Per-H), 7.81 (d, $J = 8.07$, 2H, Per-H), 7.53–7.34 (m, 20H, Car-H), 4.13–4.04 (m, 4H, N-CH₂), 1.92 (m, 2H), 1.38–1.30 (m, 16H), 0.94–0.88 (m, 12H). ^{13}C NMR (75 MHz, CDCl_3 , δ ppm): 163.9, 163.6, 142.0, 141.75, 141.72, 139.8, 137.2, 135.6, 135.1, 132.7, 130.2, 130.0, 129.3, 129.2, 127.7, 127.5, 126.7, 123.5, 122.8, 122.0, 121.7, 121.1, 120.57, 120.54, 110.1, 109.9, 44.2, 37.9, 30.7, 28.7, 24.0, 23.1, 14.1, 10.6. FAB-MASS (+VE): (*m/z*) 1097.496.

Anal. Calcd for $\text{C}_{76}\text{H}_{64}\text{N}_4\text{O}_4$: C, 83.18; H, 5.88; N, 5.11. Found: C, 82.98; H, 5.77; N, 4.98.

CONCLUSIONS

A series of donor–acceptor systems of substituted perylenediimides with an extended π -system were synthesized. All regioisomers of 1,6- and 1,7-disubstituted PDIs were separated using conventional column chromatography and characterized. A red shift in the absorbance maxima of 1,7-regiomers was observed as compared to 1,6-regiomers. No significant differences in electrochemical properties of 1,6- and 1,7-disubstituted PDIs were observed. Thermal properties such as melting point, glass transition temperature, and crystallization temperature of regiomers were found to be different, while retaining the high thermal stabilities of perylenediimides. It is clear that energy levels of 1,6- and 1,7-regiomers did not differ greatly, so the applications where the energy levels were considered may not be affected. The photovoltaic and organic field effect transistor studies are underway in our laboratory.

ASSOCIATED CONTENT

S Supporting Information

^1H NMR, ^{13}C NMR, and TGA data and geometry optimized structures for all compounds. This material is available free of charge via the Internet at <http://pubs.acs.org>.

AUTHOR INFORMATION

Corresponding Author

*Phone: (+65) 65164327. Fax: (+65) 67791691. E-mail: chmsv@nus.edu.sg.

Notes

The authors declare no competing financial interest.

ACKNOWLEDGMENTS

We gratefully acknowledge the support of Department of Chemistry, National University of Singapore, for providing facilities and NUS computer center for high performance computation. A.K. thanks NUS NanoCore for a graduate scholarship.

REFERENCES

- Quante, H.; Geerts, Y.; Mullen, K. *Chem. Mater.* **1997**, *9*, 495.
- Thelakkat, M.; Pösch, P.; Schmidt, H.-W. *Macromolecules* **2001**, *34*, 7441.
- Li, C.; Liu, M.; Pschirer, N. G.; Baumgarten, M.; Müllen, K. *Chem. Rev.* **2010**, *110*, 6817.
- Huang, C.; Barlow, S.; Marder, S. R. *J. Org. Chem.* **2011**, *76*, 2386.
- Scholz, M.; Schmidt, R.; Krause, S.; Schöll, A.; Reinert, F.; Würthner, F. *Appl. Phys. A: Mater. Sci. Process.* **2009**, *95*, 285.
- Liang, B.; Zhang, Y.; Wang, Y.; Xu, W.; Li, X. *J. Mol. Struct.* **2009**, *917*, 133.
- Vajiravelu, S.; Lygaitis, R.; Grazulevicius, J. V.; Gaidelis, V.; Jankauskas, V.; Valiyaveettil, S. *J. Mater. Chem.* **2009**, *19*, 4268.
- Chen, S.; Liu, Y.; Qiu, W.; Sun, X.; Ma, Y.; Zhu, D. *Chem. Mater.* **2005**, *17*, 2208.
- Edvinsson, T.; Li, C.; Pschirer, N.; Schöneboom, J.; Eickemeyer, F.; Sens, R.; Boschloo, G.; Herrmann, A.; Müllen, K.; Hagfeldt, A. *J. Phys. Chem. C* **2007**, *111*, 15137.
- Balaji, G.; Kale, T. S.; Keerthi, A.; Della Pelle, A. M.; Thayumanavan, S.; Valiyaveettil, S. *Org. Lett.* **2011**, *13*, 18.
- Ego, C.; Marsitzky, D.; Becker, S.; Zhang, J.; Grimsdale, A. C.; Müllen, K.; MacKenzie, J. D.; Silva, C.; Friend, R. H. *J. Am. Chem. Soc.* **2003**, *125*, 437.
- Würthner, F.; Thalacker, C.; Diele, S.; Tschiesske, C. *Chem.—Eur. J.* **2001**, *7*, 2245.

- (13) Posch, P.; Thelakkat, M.; Schmidt, H. W. *Synth. Met.* **1999**, *102*, 1110.
- (14) Seo, H.-S.; An, M.-J.; Zhang, Y.; Choi, J.-H. *J. Phys. Chem. C* **2010**, *114*, 6141.
- (15) Costa, R. D.; Cespedes-Guirao, F. J.; Ortí, E.; Bolink, H. J.; Gierschner, J.; Fernandez-Lazaro, F.; Sastre-Santos, A. *Chem. Commun.* **2009**, 3886.
- (16) Costa, R. N. D.; Cespedes-Guirao, F. J.; Bolink, H. J.; Fernández-Lázaro, F.; Sastre-Santos, Á.; Ortí, E.; Gierschner, J. *J. Phys. Chem. C* **2009**, *113*, 19292.
- (17) Cespedes-Guirao, F. J.; García-Santamaría, S.; Fernández-Lázaro, F.; Sastre-Santos, A.; Bolink, H. J. *J. Phys. D: Appl. Phys.* **2009**, *42*, 105106.
- (18) Calzado, E. M.; Villalvilla, J. M.; Boj, P. G.; Quintana, J. A.; Gómez, R.; Segura, J. L.; Díaz-García, M. A. *J. Phys. Chem. C* **2007**, *111*, 13595.
- (19) Díaz-García, M. A.; Calzado, E. M.; Villalvilla, J. M.; Boj, P. G.; Quintana, J. A.; Cespedes-Guirao, F. J.; Fernández-Lázaro, F.; Sastre-Santos, Á. *Synth. Met.* **2009**, *159*, 2293.
- (20) Schmidt-Mende, L.; Fechtenkötter, A.; Mullen, K.; Moons, E.; Friend, R. H.; MacKenzie, J. D. *Science* **2001**, *293*, 1119.
- (21) Jeong, S.; Han, Y. S.; Kwon, Y.; Choi, M.-S.; Cho, G.; Kim, K.-S.; Kim, Y. *Synth. Met.* **2010**, *160*, 2109.
- (22) Planells, M.; Cespedes-Guirao, F. J.; Goncalves, L.; Sastre-Santos, A.; Fernandez-Lazaro, F.; Palomares, E. *J. Mater. Chem.* **2009**, *19*, 5818.
- (23) Planells, M.; Cespedes-Guirao, F. J.; Forneli, A.; Sastre-Santos, A.; Fernandez-Lazaro, F.; Palomares, E. *J. Mater. Chem.* **2008**, *18*, 5802.
- (24) O'Neil, M. P.; Niemczyk, M. P.; Svec, W. A.; Gosztola, D.; Gaines, G. L. III; Wasielewski, M. R. *Science* **1992**, *257*, 63.
- (25) Chen, Z.; Debije, M. G.; Debaerdemaecker, T.; Osswald, P.; Würthner, F. *ChemPhysChem* **2004**, *5*, 137.
- (26) Jones, B. A.; Ahrens, M. J.; Yoon, M. H.; Facchetti, A.; Marks, T. J.; Wasielewski, M. R. *Angew. Chem., Int. Ed.* **2004**, *43*, 6363.
- (27) Guo, X.; Zhang, D.; Zhu, D. *Adv. Mater.* **2004**, *16*, 125.
- (28) Baffreau, J.; Leroy-Lhez, S.; Ván Anh, N.; Williams, R.; Hudhomme, P. *Chem.—Eur. J.* **2008**, *14*, 4974.
- (29) He, X.; Liu, H.; Li, Y.; Wang, S.; Wang, N.; Xiao, J.; Xu, X.; Zhu, D. *Adv. Mater.* **2005**, *17*, 2811.
- (30) Wang, B.; Yu, C. *Angew. Chem., Int. Ed.* **2010**, *49*, 1485.
- (31) Cespedes-Guirao, F. J.; Ropero, A. B.; Font-Sanchis, E.; Nadal, A.; Fernandez-Lazaro, F.; Sastre-Santos, A. *Chem. Commun.* **2011**, *47*, 8307.
- (32) Peneva, K.; Mihov, G.; Herrmann, A.; Zarabi, N.; Börsch, M.; Duncan, T. M.; Müllen, K. *J. Am. Chem. Soc.* **2008**, *130*, 5398.
- (33) Kelley, R. F.; Shin, W. S.; Rybtchinski, B.; Sinks, L. E.; Wasielewski, M. R. *J. Am. Chem. Soc.* **2007**, *129*, 3173.
- (34) Wasielewski, M. R. *Acc. Chem. Res.* **2009**, *42*, 1910.
- (35) You, C. C.; Hippius, C.; Grüne, M.; Würthner, F. *Chem.—Eur. J.* **2006**, *12*, 7510.
- (36) Cespedes-Guirao, F. J.; Martín-Gomis, L.; Ohkubo, K.; Fukuzumi, S.; Fernández-Lázaro, F.; Sastre-Santos, Á. *Chem.—Eur. J.* **2011**, *17*, 9153.
- (37) Cespedes-Guirao, F. J.; Ohkubo, K.; Fukuzumi, S.; Fernández-Lázaro, F.; Sastre-Santos, Á. *Chem. Asian J.* **2011**, *6*, 3110.
- (38) Cespedes-Guirao, F. J.; Ohkubo, K.; Fukuzumi, S.; Sastre-Santos, A.; Fernández-Lázaro, F. *J. Org. Chem.* **2009**, *74*, 5871.
- (39) Wasielewski, M. R. *J. Org. Chem.* **2006**, *71*, 5051.
- (40) Würthner, F. *Chem. Commun.* **2004**, 1564.
- (41) Tan, Z. A.; Zhou, E.; Zhan, X.; Wang, X.; Li, Y.; Barlow, S.; Marder, S. R. *Appl. Phys. Lett.* **2008**, *93*, 73309.
- (42) Zhou, E.; Tajima, K.; Yang, C.; Hashimoto, K. *J. Mater. Chem.* **2010**, *20*, 2362.
- (43) Reghu, R. R.; Bisoyi, H. K.; Grazulevicius, J. V.; Anjukandi, P.; Gaidelis, V.; Jankauskas, V. *J. Mater. Chem.* **2011**, *21*, 7811.
- (44) Battagliarin, G.; Li, C.; Enkelmann, V.; Müllen, K. *Org. Lett.* **2011**, *13*, 3012.
- (45) Nakazono, S.; Easwaramoorthi, S.; Kim, D.; Shinokubo, H.; Osuka, A. *Org. Lett.* **2009**, *11*, S426.
- (46) Bullock, J. E.; Vagnini, M. T.; Ramanan, C.; Co, D. T.; Wilson, T. M.; Dicke, J. W.; Marks, T. J.; Wasielewski, M. R. *J. Phys. Chem. B* **2010**, *114*, 1794.
- (47) Kamm, V.; Battagliarin, G.; Howard, I. A.; Pisula, W.; Mavrinskiy, A.; Li, C.; Müllen, K.; Laquai, F. *Adv. Energy Mater.* **2011**, *1*, 137.
- (48) Ego, C.; Marsitzky, D.; Becker, S.; Zhang, J.; Grimsdale, A. C.; Müllen, K.; MacKenzie, J. D.; Silva, C.; Friend, R. H. *J. Am. Chem. Soc.* **2002**, *125*, 437.
- (49) Böehm, A.; Arms, H.; Henning, G.; Blaschka, P. (BASF AG) German Patent DE 19547209 A1, 1997.
- (50) Würthner, F.; Stepanenko, V.; Chen, Z.; Saha-Möller, C. R.; Kocher, N.; Stalke, D. *J. Org. Chem.* **2004**, *69*, 7933.
- (51) Dubey, R. K.; Efimov, A.; Lemmettyinen, H. *Chem. Mater.* **2010**, *23*, 778.
- (52) Fan, L.; Xu, Y.; Tian, H. *Tetrahedron Lett.* **2005**, *46*, 4443.
- (53) Handa, N. V.; Mendoza, K. D.; Shirtcliff, L. D. *Org. Lett.* **2011**, *13*, 4724.
- (54) Sivamurugan, V.; Kazlauskas, K.; Jursenas, S.; Gruodis, A.; Simokaitiene, J.; Grazulevicius, J. V.; Valiyaveettil, S. *J. Phys. Chem. B* **2010**, *114*, 1782.
- (55) Lai, W.-Y.; He, Q.-Y.; Chen, D.-Y.; Huang, W. *Chem. Lett.* **2008**, *37*, 986.
- (56) Medina, A.; Claessens, C. G.; Rahman, G. M. A.; Lamsabhi, A. M.; Mo, O.; Yanez, M.; Guldi, D. M.; Torres, T. *Chem. Commun.* **2008**, 1759.
- (57) Kim, S.-K.; Lee, Y.-M.; Lee, C.-J.; Lee, J.-H.; Oh, S.-Y.; Park, J.-W. *Mol. Cryst. Liq. Cryst.* **2008**, *491*, 133.
- (58) Chao, C. C.; Leung, M. K.; Su, Y. O.; Chiu, K. Y.; Lin, T. H.; Shieh, S. J.; Lin, S. C. *J. Org. Chem.* **2005**, *70*, 4323.
- (59) Tavasli, M.; Bettington, S.; Bryce, M. R.; Batsanov, A. S.; Monkman, A. P. *Synthesis* **2005**, 1619.
- (60) Frisch, M. J.; Trucks, G. W.; Schlegel, H. B.; Scuseria, G. E.; Robb, M. A.; Cheeseman, J. R.; Scalmani, G.; Barone, V.; Mennucci, B.; Petersson, G. A.; Nakatsuji, H.; Caricato, M.; Li, X.; Hratchian, H. P.; Izmaylov, A. F.; Bloino, J.; Zheng, G.; Sonnenberg, J. L.; Hada, M.; Ehara, M.; Toyota, K.; Fukuda, R.; Hasegawa, J.; Ishida, M.; Nakajima, T.; Honda, Y.; Kitao, O.; Nakai, H.; Vreven, T.; Montgomery, J. A., Jr.; Peralta, J. E.; Ogliaro, F.; Bearpark, M.; Heyd, J. J.; Brothers, E.; Kudin, K. N.; Staroverov, V. N.; Kobayashi, R.; Normand, J.; Raghavachari, K.; Rendell, A.; Burant, J. C.; Iyengar, S. S.; Tomasi, J.; Cossi, M.; Rega, N.; Millam, J. M.; Klene, M.; Knox, J. E.; Cross, J. B.; Bakken, V.; Adamo, C.; Jaramillo, J.; Gomperts, R.; Stratmann, R. E.; Yazayev, O.; Austin, A. J.; Cammi, R.; Pomelli, C.; Ochterski, J. W.; Martin, R. L.; Morokuma, K.; Zakrzewski, V. G.; Voth, G. A.; Salvador, P.; Dannenberg, J. J.; Dapprich, S.; Daniels, A. D.; Farkas, O.; Foresman, J. B.; Ortiz, J. V.; Cioslowski, J.; Fox, D. J. *Gaussian 09*, revision A.02; Gaussian, Inc.: Wallingford, CT, 2009.
- (61) Dennington, R.; Keith, T.; Millam, J. *GaussView*, version 5; Semichem Inc.: Shawnee Mission, KS, 2009.